PERFORMANCE OF AlGaN/GaN HETEROSTRUCTURE FIELD–EFFECT TRANSISTORS FOR HIGH–FREQUENCY AND HIGH–POWER ELECTRONICS

P. Kordoš[1,2,3], J. Bernát[3], G. Heidelberger[3], and M. Marso[3]

[1]*Institute of Electrical Engineering, Slovak Academy of Sciences, SK-84104 Bratislava, Slovakia*
Phone: +4212-5477-5806, Fax:+4212-5477-5816, E-mail: elekkord@savba.sk
[2]*Department of Microelectronics, Slovak Technical University, SK-81219 Bratislava, Slovakia*
[3]*Institute of Thin Films and Interfaces and cni – Center of Nanoelectronic Systems for Information Technology, Research Centre Jülich, D-52425 Jülich, Germany*

Summary Preparation and properties of GaN–based heterostructure field–effect transistors (HFETs) for high–frequency and high–power applications are studied in this work. Performance of unpassivated and SiO_2 passivated AlGaN/GaN HFETs, as well as passivated SiO_2/AlGaN/GaN MOSHFETs (metal–oxide–semiconductor HFETs) is compared. It is found that MOSHFETs exhibit better DC and RF properties than simple HFET counterparts. Deposited SiO_2 yielded an increase of the sheet carrier density from 7.6×10^{12} cm^{-2} to 9.2×10^{12} cm^{-2} and subsequent increase of the static drain saturation current from 0.75 A/mm to 1.09 A/mm. Small–signal RF characterisation of MOSHFETs showed an extrinsic current gain cut-off frequency f_T of 24 GHz and a maximum frequency of oscillation f_{max} of 40 GHz. These are fully comparable values with state-of-the-art AlGaN/GaN HFETs. Finally, microwave power measurements confirmed excellent performance of MOSHFETs: the output power measured at 7 GHz is about two–times larger than that of simple unpassivated HFET. Thus, a great potential in application of GaN-based MOSHFETs is documented.

1. INTRODUCTION

It is well known that future devices used in new communication systems need to operate simultaneously at higher frequencies (higher speed, larger bandwidth) and higher powers. Unfortunately, Si–based and GaAs–based devices cannot fulfil this requirement, as it follows from their fundamental material and electronic transport parameters. Schematic frequency vs power diagram for devices using various semiconductor materials is shown in Fig. 1 [1]. Materials with higher bandgap, such as SiC and GaN (3.4 eV), clearly dominate. However, the natural advantage of GaN over SiC is the possibility of making heterostructures using AlGaN, InGaN or InAlN. Since recently GaN–based transistors are under systematic study by various academic and industry research groups. An expressive progress concerning the preparation and performance of AlGaN/GaN heterostructure field–effect transistors (HFETs) can be observed [2]. This can be demonstrated by recently reported total output power of 179 W at 2 GHz on 48 mm wide (i.e. 3.7 W/mm power density) single-chip HFET by Device Research Labs of NEC Corp. [3]. In spite of these record power data they are still some material and device issues, which need to be solved concerning mass production and wide application of AlGaN/GaN HFET devices. One key problem at the preparation of GaN-based devices is the lack of native substrates [4]. The material structure needs to be grown as lattice-mismatched to the substrate such as sapphire, Si or SiC. High gate leakage currents and DC/RF drain current dispersion, which limit microwave output power, as well as performance degradation belong to the main questions concerning the device preparation. Various tasks such as material structure optimisation [5], dielectric passivation [6] and field-modulating gate plate [7] are used to suppress or eliminate these effects. Recently an application of gate insulator, i.e. preparation of MISHFET devices, has been shown as a perspective alternative for the preparation of reliable GaN–based transistors [8].

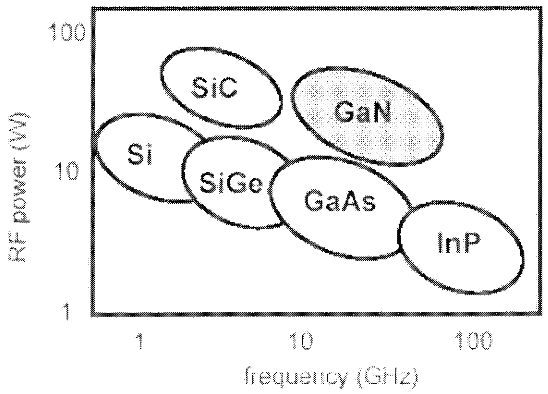

Fig. 1. Schematic frequency vs power diagram for devices on various semiconductor materials [1]

In this paper, an influence of a SiO_2 insulator, deposited on the ungated surface access region as well as below the gate, on the performance of AlGaN/GaN HFETs is investigated. The DC and RF performance of unpassivated and passivated HFETs and passivated MOSHFETs, prepared on the same material structure, is compared. It is shown that SiO_2 passivated MOSHFETs exhibit higher output power than simultaneously prepared Schottky-gate HFET counterparts.

2. DEVICE PREPARATION

Experimental basis for the study reported here was the simultaneous fabrication of unpassivated and SiO_2 passivated AlGaN/GaN HFETs and SiO_2 gate insulator AlGaN/GaN MOSHFETs. The material structure for all devices consisted of 3 μm thick undoped GaN and 30 nm thick undoped $Al_{0.28}Ga_{0.72}N$ layers grown on insulating 4H-SiC substrate by LP-MOCVD (Cree-GaN Durham). The device processing consisted of conventional FET fabrication steps. At first mesa etching isolation using argon sputtering was performed. After that ohmic contacts were prepared by evaporating multilayered Ti/Al/Ni/Au sequence followed by rapid thermal annealing at 850 °C for 30 s in a N_2 ambient. The ohmic contact resistance of 0.22–0.35 Ω mm was measured using the transmission-line-method. The Schottky gate metallization consisted of a Ni/Au double-layer patterned by e-beam lithography. Devices with a gate length of 0.3 - 0.9 μm and a gate width of 100 μm and 200 μm (two fingers) were prepared. Van der Pauw patterns with an active area of 0.3×0.3 mm^2 were processed simultaneously with HFET devices. A SiO_2-layer of 10 nm nominal thickness was deposited by PECVD to fabricate the passivated HFETs. To prepare the MOSHFETs, the same oxide-thickness was chosen as for passivated HFETs and PECVD was applied as well.

3. SiO_2/AlGaN/GaN HETEROSTRUCTURE CHARACTERISATION

The material structure was characterized by Hall effect measurements on van der Pauw patterns and C–V measurements on HFET devices itself. It is well known that dielectric passivation of AlGaN/GaN heterostructure compensates surface states and thus induces an increase of the sheet carrier density in the 2DEG channel [9]. This effect was confirmed on our samples investigated. Hall effect data yielded a sheet carrier density of 7.14×10^{12} cm^{-2} and 9.25×10^{12} cm^{-2} and a carrier mobility of 1835 cm^2/Vs and 1670 cm^2/Vs on unpassivated and SiO_2-passivated material structures, respectively. The passivation induced sheet carrier density $\Delta n_s = 2.1\times10^{12}$ cm^{-2} and partial decrease of the mobility are in good agreement with our previous investigations ($\Delta n_s = 1.5\times10^{12}$ cm^{-2} after Si_3N_4-passivation) [9].

Figure 2 shows the capacitance–voltage characteristics typical for unpassivated AlGaN/GaN HFET and passivated SiO_2/AlGaN/GaN MOSHFET. The C–V curves show sharp transitions and negligible hysteresis. The sheet carrier density can be evaluated from the capacitance and threshold voltage as

$$n_s = (C_n \times V_{th})/q. \qquad (1)$$

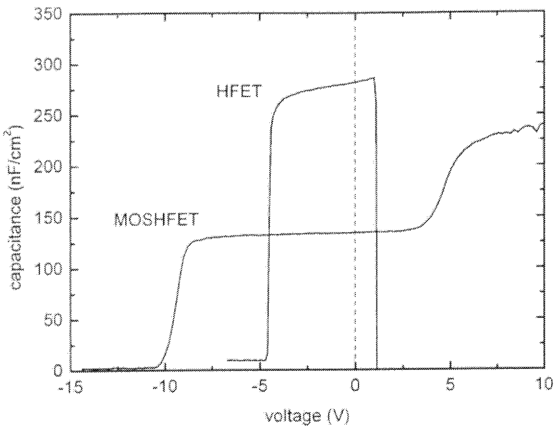

Fig. 2 Capacitance–voltage characteristics of unpassivated AlGaN/GaN HFET and passivated SiO_2/AlGaN/GaN MOSHFET

Values of 7.6×10^{12} cm^{-2} and 9.2×10^{12} cm^{-2} for unpassivated HFET and passivated MOSHFET, respectively, are in excellent agreement with mentioned above Hall data. Similarly, from the zero-bias capacitance of HFET we can evaluate the AlGaN thickness $d_{AlGaN} = \varepsilon/C = 29.4$ nm, comparing to the nominal thickness of 30 nm. From the zero-bias capacitances of HFET and MOSHFET considering that

$$C_{HFET}/C_{MOSHFET} = [1 + (d_{SiO2}/d_{AlGaN})(\varepsilon_{AlGaN}/\varepsilon_{SiO2})], \qquad (2)$$

and using AlGaN and SiO_2 layer permitivities ε = 9.2 and 3.9 respectively, we extracted the SiO_2 thickness of 12 nm. The nominal thickness of SiO_2 was 10 nm. A saturation of the MOSHFET capacitance at higher gate voltages indicates that the capacitance of SiO_2 insulator only is measured. Our preliminary evaluation of the SiO_2 surface states density from the single-frequency capacitance and conductance measurements indicates that $D_{SS} = 1.1\times10^{12}$ cm^{-2} eV^{-1}. This is in good agreement with results published before on SiO_2/GaN structures [10].

4. DEVICE PERFORMANCE

It is well known that AlGaN/GaN HFETs exhibit relatively high gate leakage currents. For simple undoped and unpassivated AlGaN/GaN heterostructure, as used here, the gate leakage currents of about 10^{-6} A/mm ($V_G = -6$ V) are usually observed. They can be about one order of magnitude lower if passivation is used. We reported recently that another alternative to suppress the gate current is by using undoped GaN cap on top of the heterostructure, which enhances the Schottky barrier height [5]. Leakage currents of about 10^{-8} A/mm were found on unpassivated GaN/AlGaN/GaN devices. Figure 3 (full lines) shows typical two

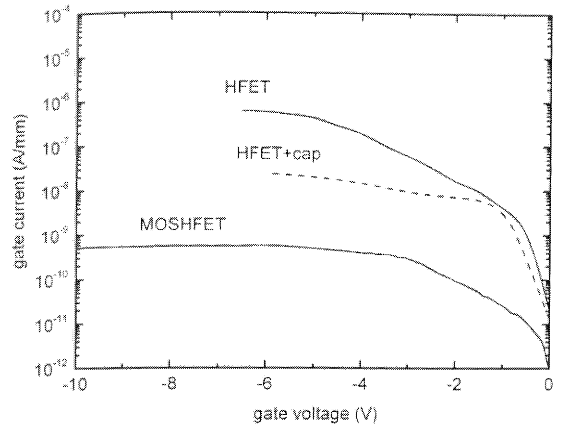

Fig. 3 Two terminal gate–source I–V characteristics of unpassivated AlGaN/GaN HFET and passivated SiO_2/AlGaN/GaN MOSHFET

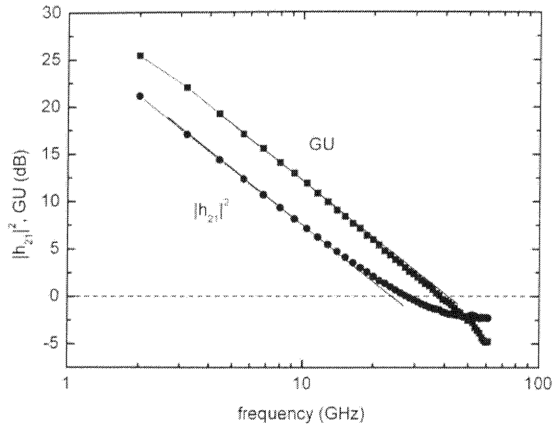

Fig. 5 Small signal performance of passivated SiO_2/AlGaN/GaN MOSHFET with 0.7 μm and 200 μm gate length and width, respectively

terminal gate–source I–V characteristics of unpassivated HFET and passivated MOSHFET. The data for HFET with GaN cap [5] are shown for comparison too (dashed line). Very low gate currents, ~5×10^{-10} A/mm at $V_G \leq -6$ V,were measured on SiO_2/AlGaN/GaN MOSHFETs. Nearly identical currents, 7×10^{-10} A/mm at $V_G = -10$ V, were reported before if Si_3N_4 gate insulator was used [11].

Typical static output characteristics of AlGaN/GaN MOSHFETs are shown in Fig. 4. Low output conductance and minimal thermal effects are observed. A drain saturation current of 1.09 A/mm is obtained at 1 V on the gate. This is comparable value to that known on state-of-the-art passivated AlGaN/GaN HFETs. The threshold voltage is close to –11 V opposed to about –6 V observed commonly on HFETs. This is expected due to additional serial capacitance of the insulator and as it follows from the C-V measurements (Fig. 2). Thus, the peak extrinsic transconductance g_m of 118 mS/mm is slightly lower than reported on HFETs. For comparison, a drain saturation current of 0.75 A/mm and a peak extrinsic transconductance of 165 mS/mm were found on unpassivated HFETs processed simultaneously on similar AlGaN/GaN material structure.

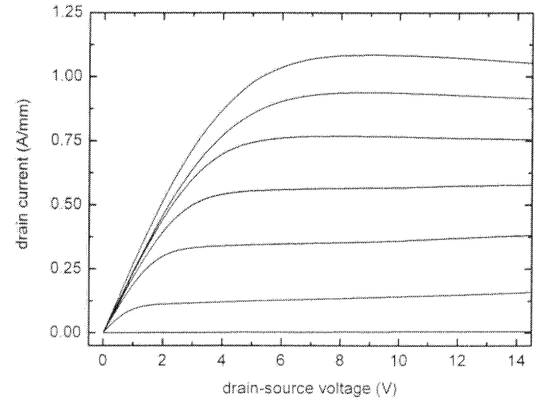

Fig.4 Output characteristics of SiO_2*/AlGaN/GaN MOSHFET ($V_{G,\,top} = 1$ V, $\Delta V_G = -2$ V)*

Small signal RF characterisation of the devices was carried out by on-wafer S-parameter measurements up to 60 GHz. Figure 5 shows an example of the short circuit current gain (h_{21}) and the unilateral power gain (GU) as a function of frequency for SiO_2/AlGaN/GaN MOSHFET with 0.7 μm and 200 μm gate length and width, respectively. An extrinsic current gain cut-off frequency f_T of 24 GHz and a maximum frequency of oscillation f_{max} of 40 GHz are evaluated from these data measured at $V_{DS} = 15$ V and $V_G = -7$ V biases. These are fully comparable values with those reported on state-of-the-art AlGaN/GaN HFETs. The $f_T \times L_G$ product of 16.8 GHz μm is even slightly higher than commonly reported for AlGaN/GaN HFETs [12]. This follows from lower decrease of the transconductance than of the gate capacitance for MOSHFET comparing to HFET (f_T is proportional to the ratio of g_m and C_G). The cut-off frequency ratio $f_{max}/f_T = 1.7$ is a reasonable value. All these, i.e. static and small-signal microwave performance of MOSHFET devices prepared, indicate on a good quality of used SiO_2 without degradation of the carrier mobility in the channel. Thus, a great potential in application of GaN-based MOSHFETs is documented.

Finally, microwave power measurements were performed using an on-wafer load pull measurement system. Output power sweeps of these devices were conducted at 7 GHz. Impedance matching was accomplished with automatically–adjusted tuners. The devices were biased to an V_G,V_D–point which corresponds to the class A operation. The output power P_{out}, gain G and power–added efficiency PAE as a function of the input power P_{in} were measured and the output power density was evaluated. As expected, the peak output power increases nearly

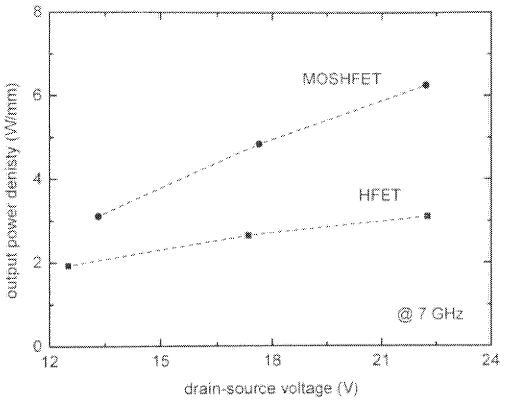

Fig. 6 Output power density at 7 GHz as a function of drain bias for passivated SiO_2/AlGaN/GaN MOSHFET and unpassivated HFET with 0.7 μm gate length

linearly with increased drain bias. This is shown in Fig. 6, in which the output power density at 7 GHz as a function of the drain voltage for unpassivated HFET and passivated MOSHFET with 0.7 μm and 200 μm gate length and width, respectively, is shown. An advantage of AlGaN/GaN MOSHFET over HFET is demonstrated clearly. The output power of MOSHFET is about two–times higher than that of HFET.

5. CONCLUSIONS

An influence of a SiO_2 insulator, deposited on the ungated surface access region as well as below the gate, on the DC and RF performance of AlGaN/GaN HFETs was investigated. It was shown that SiO_2 passivated MOSHFETs exhibit very low leakage current ($\sim 5\times10^{-10}$ A/mm at $V_G \leq -6$ V) and reasonable DC performance (the drain saturation current of 1.09 A/mm and the peak extrinsic transconductance g_m of 118 mS/mm). Small signal RF characterisation yielded cut-off frequencies f_T of 24 GHz and f_{max} of 40 GHz. The $f_T \times L_G$ product of 16.8 GHz μm is slightly higher than commonly reported for AlGaN/GaN HFETs. The main observation in this study is that the output power of MOSHFETs measured at 7 GHz is about two-times larger than that of simultaneously investigated unpassivated Schottky gate HFET. This result confirms a great potential of GaN-based MOSHFETs for high-frequency and high-power electronics.

Acknowledgements

The authors thank J. Flynn and G. Brandes from CREE GaN Inc. for providing epitaxial material according our specification. The work reported here is partially supported by Slovak Scientific Grant Agency VEGA (contracts No. 1/2041/05 and 2/3115/23).

REFERENCES

[1] Duboz J.-Y.: GaN as seen by the industry, phys. Stat. solidi (a) 176, 5 (1999).

[2] Mishra U.K., Parikh P., and Wu Y.-F.: AlGaN/GaN HEMTs – an overview of device operation and application, Proc. IEEE 90, 1022 (2002).

[3] Okamoto Y., Ando Y., Hataya K., Miyamoto M., Nakayama T., Inoue T., and Kuzuhara M.: 179 W recessed-gate AlGaN/GaN heterostructure FET with field-modulating plate, Electron. Lett. 40, 629 (2004).

[4] Kordoš P., Morvic M., Betko J., Novák J., Flynn J., and Brandes G.: Conductivity and Hall effect of freestanding highly-resistive epitaxial GaN:Fe substrates, Appl. Phys. Lett. 85, 5616 (2004).

[5] Kordoš P., Bernát J., and Marso M.: Impact of layer structure on performance of unpassivated AlGaN/GaN HEMT, J. Microelectronics, Available online 19 March (2005).

[6] Javorka P., Bernát J., Fox A., Marso M., Lüth H., and Kordoš P.: Influence of SiO_2 and Si_3N_4 passivation on performance of AlGaN/GaN/Si HEMTs, Electron. Lett. 39, 1155 (2003).

[7] Chini A., Buttari D., Coffie R., Heikman S., Keller S., and Mishra U.K.: 12 W/mm power density AlGaN/GaN HEMTs on sapphire substrate, Electron. Lett. 40, 73 (2004).

[8] Cai Y., Zhou Y.G., Chen K.J., and Lau K.M.: III-nitride MIS heterojunction field-effect transistors using sputtered AlON thin films, Appl. Phys. Lett. 86, 032109-1 (2005).

[9] Bernát J., Javorka P., Marso M., and Kordoš P.: Conductivity and Hall effect measurements on intentionally undoped and doped AlGaN/GaN heterostructures before and after passivation, App. Phys. Lett. 83, 5455 (2003).

[10] Hashizume T., Ootomo S., Inagaki T., and Hasegawa H.: Surface passivation of GaN and GaN/AlGaN heterostructures by dielectric films and its application to insulated-gate heterostructure transistors, J. Vac. Sci. Technol. B 21, 1828 (2003).

[11] Adivaran V., Gaevski M., Sun W.H., Koudymov A., Simin G., Yang J., Khan M.A., Tarakij A., Shur M.S., Gaska R. : Submicron gate Si_3N_4/AlGaN/GaN metal-insulator-semiconductor heterostructure field-effect transistor, IEEE Electron Dev. Lett. 24, 541 (2003).

[12] Kordoš P.: Material and device issues of AlGaN/GaN high electron mobility transistors, in: Handbook of Semiconductor Nanostructures and Devices, Eds.: A.A. Balandin and K.L. Wang, American Scientific Publisher, ISBN: 158883-073-X, to be publ. October 2005.